Journal of Coastal Research	00	0	000–000	Coconut Creek, Florida	Month 0000

Coastal Mangrove Squeeze in the Mekong Delta

Linh K. Phan[†‡], Jaap S.M. van Thiel de Vries[†§], and Marcel J.F. Stive[†]*

[†]Faculty of Civil Engineering and Geosciences
Delft University of Technology
Delft, The Netherlands

[‡]Faculty of Civil Engineering
Water Resources University
Ha Noi, Vietnam

[§]Royal Boskalis Westminster NV, Hydronamic
Papendrecht, The Netherlands

www.cerf-jcr.org

www.JCRonline.org

ABSTRACT

Phan, L.K.; van Thiel de Vries, J.S.M., and Stive, M.J.F., 0000. Coastal mangrove squeeze in the Mekong Delta. *Journal of Coastal Research,* 00(0), 000–000. Coconut Creek (Florida), ISSN 0749-0208.

The role of mangrove forests in providing coastal zone stability and protection against flooding is increasingly recognized. The specific root, stem, and canopy system of mangroves is highly efficient in attenuating waves and currents. The sheltered environment created by a healthy mangrove forest offers great sedimentation potential in case a sediment source is available. However, the once-abundant mangrove forests in the Mekong coastal delta are becoming rapidly depleted. Especially along the Mekong eastern and southeastern coast, mangrove degradation and rapid coastline erosion are observed at many locations. At these locations, the mangrove forests usually consist of a narrow strip only, sometimes as narrow as 100 m. This mangrove squeeze is mainly due to the construction of sea dikes in a quest for the creation of space for cultivation and the prevention of salinity intrusion. The basic assumption behind our work is that there is a critical minimum width of a coastal mangrove forest strip to keep its ability to stay stable or, once surpassing the minimum width, to promote sedimentation. The larger the width the more efficient the attenuation of waves and currents will be, offering both a successful seedling and sedimentary environment. Our analysis of available data both from literature and from satellite observations supports our basic assumption: an average critical width of 140 m is found for the southeastern and eastern Mekong Delta coast as a minimum width to sustain a healthy mangrove forest. To further our insights into the efficiency of mangrove to attenuate wave energy as a function of their width we have applied a state-of-the-art wave propagation model that includes both short and long waves. Our results confirm earlier results from the literature that short waves are indeed attenuated very rapidly over distances shorter than the critical width, but as we show for the first time infragravity waves penetrate over much larger distances. We therefore hypothesize that the decay of long waves plays a crucial role in the health of the mangrove.

ADDITIONAL INDEX WORDS: *Coastal erosion, sea dike.*

INTRODUCTION

The Mekong Deltaic River System (MDRS) in Vietnam (also known as the Cuu Long or the "Nine Dragons", because of the nine river outlets, although presently only now eight are left [see Figure 1B]) covers an area of 39,000 km^2 and is home to more than 17 million inhabitants. Although this is not very well known, this region is as populated as that of a country of similar size like the Netherlands, which is known as one of the most populated in the world. This is an important reason for the pressure on coastal land use.

The MDRS shapes its initial course at Phnom Penh, Cambodia, where the river divides into two main distributaries, the Mekong (Tien River) and the Bassac (Hau River). The Tien then divides into five and formally six main channels and the Hau into three channels to form the original Nine Dragons of the MDRS. The Mekong deltaic coast, which has progressed in the Holocene from the Cambodian border to its present position, is historically rich in sediment with an overall sedimentation of both sand and fines (silt and clay), creating a coastline of both mangrove and nonmangrove sections (Nguyen, Ta, and Tateishi, 2000). The average suspended sediment concentrations (SSC) from 1993 to 2000 reach approximately 100 mg/L, 50 mg/L, and 80 mg/L at Tan Chau, Can Tho, and My Thuan stations, respectively (Figure 1B) (Lu and Siew, 2006). Along the South China Sea, the Mekong Delta coast can be characterized respectively into the eastern zone from Tien Giang Province to Soc Trang Province featuring an estuarine environment, and the southeastern zone from Soc Trang Province to Ca Mau Cape featuring a transient tidal and coastal environment (Figure 1B).

Presently, sedimentation still prevails near the estuarine inlets (cf. Figure 1B), but due to natural and human-induced causes, erosion is occurring away from the inlets and it is anticipated that erosion will increase in the future for several reasons: the increasing number of dams in the Mekong River capturing SSC, the increasing human-induced subsidence due to groundwater extraction, and climate-change-induced sea-level rise (International Union for Conservation of Nature, 2011). The decrease of SSC and of mangrove health due to coastal mangrove squeeze is causing a high human-induced impact, which is our subject of interest. This coastal region experiences the compound impacts from climate change and human intervention most clearly. Coastal recession contributes to the loss of mangrove and land and increases salinity intrusion, creating problems for many functions, such as agriculture and aquaculture and coastal infrastructure. Although this is a very important area, the southeastern and eastern coasts are as yet quite understudied.

DOI: 10.2112/JCOASTRES-D-14-00049.1 received 15 March 2014; accepted in revision 30 June 2014; corrected proofs received 15 September 2014; published pre-print online 20 October 2014.
*Corresponding author: m.j.f.stive@tudelft.nl

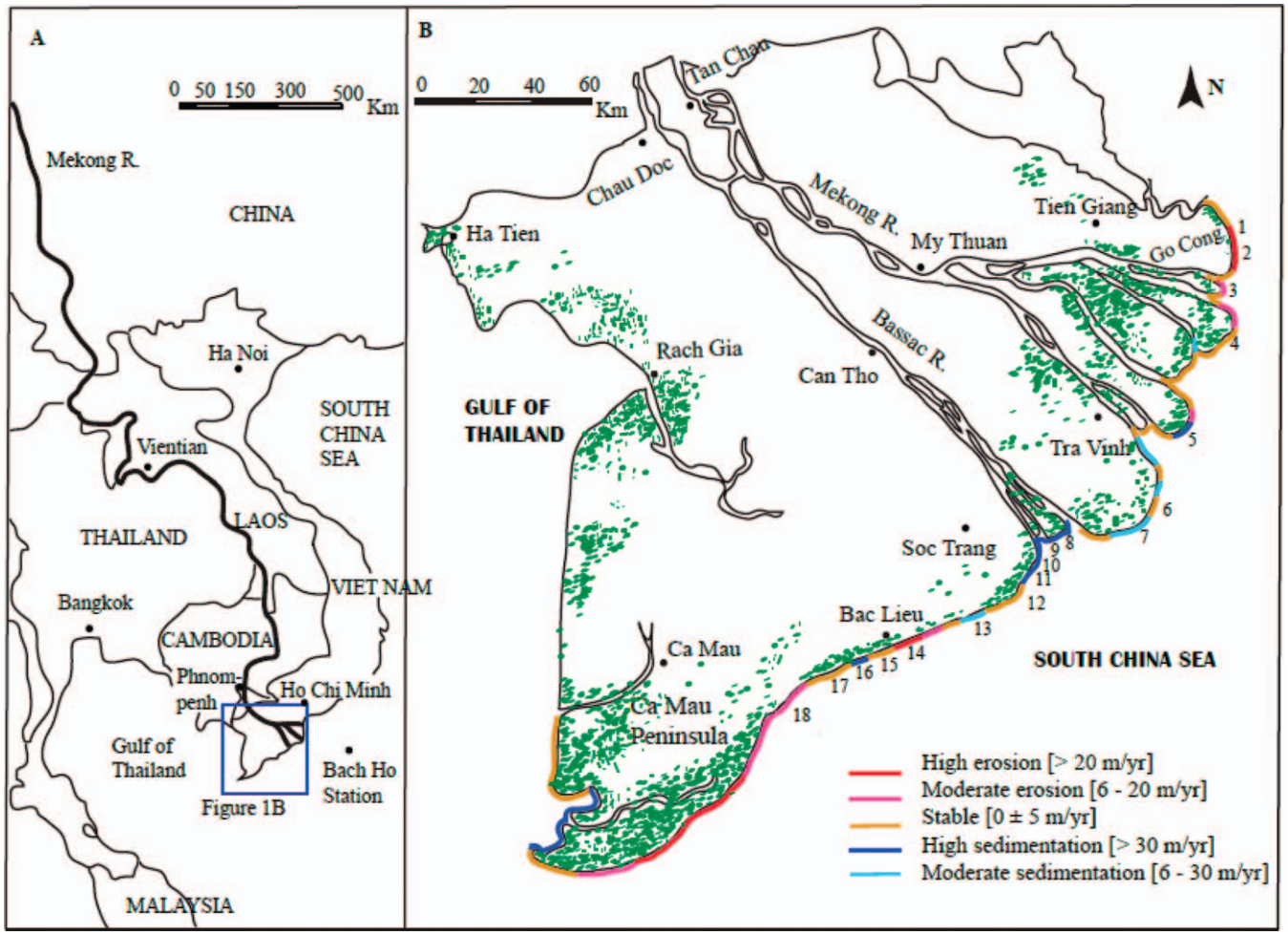

Figure 1. (A) Location of the study site in Southeast Asia. (B) Map of the Mekong Delta in Vietnam showing mangrove locations by green dots (after Spalding, Kainuma, and Collins, 2011); location of places mentioned in the text and the coastline evolution from 1989 to 2002. Places that were chosen to analyze coastline evolution in relation to mangrove space are numbered from 1 to 18. Place names are given in Table 1.

The recognition that coastal ecosystems will increase to retreat landward when relative sea level is rising has been noted abundantly in the literature (Gilman, Ellison, and Coleman, 2007). However, whenever coastal development such as urbanization, agriculture, aquaculture, and infrastructure plays a role as a blocking barrier, this will stop this migration and lead to the loss of valuable coastal habitats (Feagin *et al.*, 2010). This loss was recognized by Doody (2004) as "coastal squeeze" when this author realized the necessity of keeping space for "coastal habitats to operate". The term coastal squeeze then is used more frequently by other researchers (Gilman, Ellison, and Coleman, 2007; Torio and Chmura, 2013) when coastal habitats such as mangrove and other tidal wetlands are in danger because of sea-level rise and limiting the available space for migration landward. We therefore adopt the term "coastal mangrove squeeze" in this paper to emphasize the very same situation that is now operating on the Mekong Delta coast in Vietnam.

METHODS

After our description of the study site and the mangrove forests in their local and international context, we first present our analysis of our observations of mangrove widths and coastal behavior and compare this with existing literature. We then apply numerical process-based models to investigate in more detail the decay of both high-frequency and low-frequency wave damping. This we consider as a new addition to the research that has been done today. The low-frequency wave damping has not been considered in the international literature and we hypothesize that this is an important process that cannot be ignored.

Study Site in Global and Regional Context

Mangroves can be classified according to quite different environmental factors. On a global scale mangroves are divided into six tropical regions on the basis of their continental border: western America, eastern America, western Africa, eastern Africa, Indo-Malesia, and Australia (Duke, 1992). Vietnam

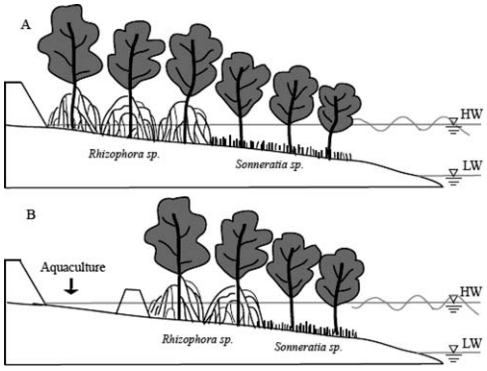

Figure 2. Two different systems of mangrove and sea dike locations along the southeastern coast and the eastern coast of MDRS. (A) Sea dikes are located right behind mangrove forest. (B) Human intervention is found in between sea dike and mangrove forest.

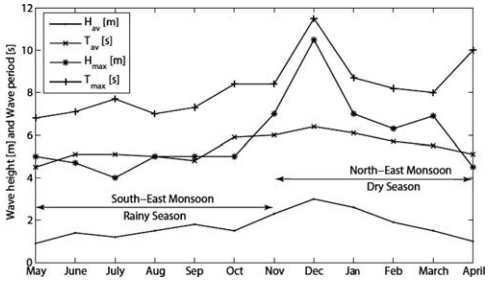

Figure 3. Monthly offshore wave parameters at Bach Ho station, situated 150 km offshore MDRS (see Fig 1A); the wave height and wave period reach their maximum value in December. Data were collected from 1986 until 2006.

belongs to the Indo-Malesian class of the most biodiverse region in the world (Alongi, 2002). Mangroves can also be defined into six classes according to their physiognomy: fringing, riverine, overwash, basin, scrub, and hammock (Lugo and Snedaker, 1974), in which coastal mangrove distributed alongshore and often exposed to waves is recognized as fringing mangrove. Woodroffe (1992) created a ternary diagram by adding the dominant physical process of tide-dominated, river-dominated, and interior mangrove into this classification. Then Ewel, Twilley, and Ong (1998) proposed a hybrid of these two systems above by referring to tide-dominated mangrove as fringe mangrove, river-dominated mangrove as riverine mangrove, and interior mangrove as basin mangrove.

According to these classifications, coastal mangrove in the MDRS can be characterized as fringe mangrove under tide dominance. It is estimated that nearly 40% of the mangrove forests in southern Vietnam were destroyed during the Vietnam War (1962–1971) (Phan and Hoang, 1993). Over 20% of about 600,000 ha of the total mangrove-forested regions of South Vietnam was defoliated in 1968 by chemical spraying. Since 1975 mangrove forests initially recovered as a result of both natural regeneration and manual planting. However, in the 1980s and early 1990s the mangrove forests were again heavily destroyed because of timber overexploitation for construction, charcoal, and conversion of forest land into aquaculture-fisheries farming systems (Christensen, Tarp, and Hjortso, 2008). By the mid-1990s forest-felling bans were imposed and the forest enterprises were forced to replant and protect the forest rather than utilize it; however, by 1999 the felling ban ceased.

Nowadays, along the eastern (locations 1 to 7) and southeastern (locations 8 to 18) coasts, there are many locations where mangrove degradations are observed. At these locations, the mangrove forests usually consist of a narrow strip only, sometimes as narrow as 100 m. This mangrove squeeze is mainly due to the construction of primary sea dikes protecting the hinterland against flooding or smaller secondary sea dikes in front of the primary sea dikes protecting aquaculture (Figure 2). Government officials usually blame the mangrove loss as well as dike collapse on sea-level rise and stronger wave action (International Union for Conservation of Nature, 2011). However, we hypothesize that mangrove squeeze due to the construction of the sea dikes is the main reason for mangrove loss and dike collapse. Subsidence due to natural causes and groundwater extraction may play a role as well. The basic assumption behind our work is that there is a critical minimum width of a coastal mangrove forest strip to keep its ability to stay stable or, once surpassing the minimum width, to promote sedimentation. The larger the width the more efficient the attenuation of waves and currents will be, offering a successful environment for both propagules and sedimentation.

The MDRS and its directly adjacent coasts have historically been under the influence of both the freshwater discharge and the actions of the tide. The freshwater discharge is very high during the flood season, especially during September and October, with an average maximum flow rate of 25,500 m^3/s, whereas during the relatively long dry season the flow is quite low, with an average lowest monthly discharge of about 2300 m^3/s in April (Tri, 2012). Especially in the dry season the tidal flows dominate. Tides in this region of the South China Sea have a semidiurnal character with a high range (more than 2 m at mean tide, increasing to 4 m at spring tide). As the tidal range decreases toward Ca Mau Cape, the number of diurnal tidal days and the diurnal characteristics increase, causing the tide to display a more diurnal than semidiurnal appearance. This is due to nonlinear interactions caused by the impact of the large shelf width on the tidal characteristics.

Although the coastal environment of the MDRS is traditionally classified as a tide-dominated environment this system is increasingly more influenced by waves as the SSCs discharged by the Mekong River are observed to decrease, which increases the impact of waves (Ta *et al.*, 2002). Offshore winds and waves at the East Sea are measured at some 150 km offshore at Bach Ho station (Figure 1A) (Hoang and Nguyen, 2006). In winter (November to April) the NE monsoon is dominating and blowing from NE to SW; in summer (May to October) the SW monsoon is dominating and blowing from SW to NE. On the basis of the observed data, the average and maximum wave heights (H_{av}, H_{max}) and wave period (T_{av}, T_{max}) for every month at Bach Ho station can be observed in Figure 3. In the dry season, the highest wave height and period are 10.5 m and 11.5

Figure 4. Google Earth images showing mangrove occurrence in front of a sea dike at different locations along the southern coast of Vietnam in 2006. The red line represents the location of the primary sea dike. (A) Mangrove consisting of a very thin strip of about 100 m in front of a primary sea dike; (B) mangrove virtually gone in front of a primary sea dike; (C) mangrove in front of the primary sea dike and protected by a secondary sea dike protecting a 300-m-wide area used for aquaculture.

seconds, respectively. At this time strong wave energy with waves of 4-m significant height occur, whereas in the rainy season, wave heights are not larger than 3 m and T_s= 5–12 seconds. Although the waves offshore can be very high, we will show later in our modelling approach that the very gentle slopes of the foreshore cause a strong damping of the wave heights to arrive inshore. This also implies that annual variations in the wave data need not be considered.

Observations of Mangrove Width and Coastline Evolution

In this section we investigate our hypothesis that once mangrove width is under squeeze, *i.e.* when either the primary or the secondary dike is too close to the nonvegetated foreshore, erosion is usually occurring and the health of the mangrove forest is under stress (see Figure 2 showing an illustrated schematization). The sections that we have chosen are near the estuarine inlets, so that sediment availability should not be a limiting factor. These two systems are found both along the southeastern coast and the eastern coast.

The first system is Google-illustrated at Go Cong 1 and 2 (Figures 4A and B; Vinh Trach Dong and Ganh Hao), where the primary sea dike is located right in front of the squeezed mangrove forest. In the second system, human interventions are found between the sea dikes and the mangrove forest. Kinh Ba is an example of the second system where about 300-m width in between the sea dike and the mangrove forest is used for aquaculture (Figure 4C). To have land protected for cultivation, a smaller and discontinuous sea dike is constructed between the aquaculture area and the mangrove forest.

We have chosen to include observations from those regions where we infer that a sediment source is still available because of the near presence of the riverine outflow, so that sediment availability is not a limiting factor. These observations are taken at different locations that undergo either erosion or sedimentation from Go Cong to Ganh Hao (chosen locations are numbered from 1 to 18 in Figure1B; location names can be found in Table 1). According to the scale classification of shores and shoreline variability presented by Stive *et al*. (2002), we are interested in evolutional trends based on the middle term scale with a timescale from years to decades and a space scale from 1 to 5 km. On the basis of the observations the typical length scale along which the rate of erosion or sedimentation can be considered rather similar is about 2 km. Ca Mau Peninsula is not considered since no sea dikes are built along the coastline of this area. The rate of coastline evolution is calculated on the basis of the shoreline evolution maps provided by the Southern Institute of Water Resources Research (2005). The evolution rates presented in Table 1 are calculated for two periods, from 1965 to 1989 and from 1989 to 2002. For each of the locations the estimated mangrove width in 2002 is also presented in Table 1. The mangrove widths, measured from Google Earth for the year 2006, were converted to 2002 by using the observed accretion and sedimentation rates. The error term involved in using this approach is not so much due to ground-referencing errors (the location of the primary or secondary sea dike is not influenced by water levels, for instance), but rather due to alongshore variability over the considered stretches that we have included in our data presentation (the horizontal error bars in Figure 5).

Before presenting our relation between coastal evolution and mangrove width, we first reflect on the erosion and accretion observations over the two periods. In the period 1965–1989 five (1, 2, 10, 12, and 18) of the 18 stretches experienced erosion. In the period 1989–2002 also five (1, 2, 3, 14, and 18) stretches experienced erosion; hence there exists variability. However, in general the erosive stretches experienced more erosion, whereas some stretches turned from stability to erosion. We refrain from making a general statement on the nature of the coastal evolution, realizing that this is also related to the supply of sediment from the MDRS and now present the relation between coastal evolution and mangrove widths.

Our suggested relationship between mangrove widths and the southeastern and the eastern coastline evolution is presented in Figure 5. In this figure the vertical axis shows the evolution rate from 1989 to 2002 (since our mangrove width observations are from 2002) and the horizontal axis shows the mangrove width. The uncertainty bars are applied in both vertical and horizontal directions. The vertical bar presents the

Table 1. *Coastal evolution rate over two periods of observation and Google-based estimated mangrove widths in 2002 at different locations along the southeastern coast and the eastern coast of the MDRS.*

		1965–1989		1989–2002		Mangrove Width (m) Converted to 2002	
No.	Cross-Section	Coastline Change (m)	Evolution Rate (m/yr)	Coastline Change (m)	Evolution Rate (m/yr)	Range (m)	Representative Value (m)
1	Go Cong 1	−250	−10	−350	−25	160–260	240
2	Go Cong 2	−350	−15	−300	−20	—	90
3	Phu Tan	2500	105	−130	−10	—	40
4	Binh Dai	1200	50	0	0	30–40	30
5	Thanh Phu	600	25	900	70	320–570	520
6	Tra Vinh 1	0	0	0	0	30–70	50
7	Tra Vinh 2	0	0	130	10	0–50	0
8	Cu Lao 1	900	40	650	50	600–750	700
9	Cu Lao 2	1800	75	1000	80	740–890	790
10	Kinh Ba 1	−350	−15	550	40	380–530	480
11	Kinh Ba 2	0	0	1000	80	440–590	540
12	Vinh Hai	−280	−10	0	0	150–250	200
13	Vinh Chau	0	0	350	25	190–290	240
14	Vinh Trach Dong 1	0	0	−350	−25	160–290	260
15	Vinh Trach Dong 2	0	0	0	0	200–300	250
16	Vinh Loi 1	700	30	600	45	420–570	515
17	Vinh Loi 2	1600	65	0	0	100–300	200
18	Ganh Hao	−200	−15	−130	−10	140–240	190

uncertainty in determining the evolution rate, on average 5 m/yr, which is at most half but often much less than half the observed rate. The horizontal bar presents the uncertainty in quantifying the mangrove width. It is based on the range of the mangrove width that is measured within 2 km (Table 1). A linear trend line is added to show the tendency of the relationship.

Although the interpretation of the results is somewhat subjective, we deduce from Figure 5 that the shoreline will remain stable with the presence of approximately 30- to 250-m width of the mangrove forest, with an average value of 140 m. A larger width will lead to a higher sedimentation potential.

However, the coastline evolution also depends on many other factors such as sediment supply, hydraulic conditions (wave, wind, current), bathymetry, *etc*. Therefore, there is no unique critical mangrove width value that can be set for all shorelines. For instance, there will be a difference between the critical mangrove width of the southeastern coast and the eastern coast and that of the west coast. Even though the West Sea has smaller tidal amplitudes and smaller wave heights, the sediment supply in the West Sea is also weaker than in the South China Sea. Therefore, no significant erosion is observed along the west coast, nor is there much sedimentation found even at the location where the mangrove forest width is about 900 m. The quantitative relationship that we provide will therefore only be applicable for the southeastern coast and the eastern coast of the Mekong Delta, although the general principle will apply to many mangrove coasts.

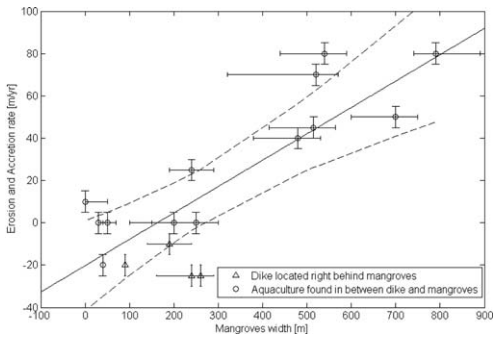

Figure 5. Relationship between mangrove width and coastline evolution along the east coast of the MDR, showing the best fit and the 90% confidence interval.

Wave Attenuation as a Function of Mangrove Forest Width

We conjecture that the health of a coastal mangrove forest is determined by its effectiveness to attenuate wave energy, which is obviously related to its width. The purpose of this section is to achieve insight into the wave transformation in the mangrove forest and suggest a rough estimation for the necessary distance from the sea dike to the mangrove forests along the southern coast of Vietnam in relation to the wave attenuation. To further our insights into the efficiency of mangrove to attenuate wave energy as a function of their width we have applied a state-of-the-art wave propagation model that includes both short and long waves. On the basis of bathymetric maps available at Delft University of Technology's map room, Soc Trang coast is chosen to present a typical coastline profile in the southern coast of Vietnam. The foreshore of the southern coast of Vietnam has a quite gentle slope (1/30,000). The water depth reaches 30 m at a distance of about 100 km offshore. Along this coast, mangroves are found to display a healthy development when a magnitude order of more than 1000-m width is present.

Mangrove Cross-Shore Distribution

For our modeling purposes we need to define more precisely our assumptions on mangrove cross-shore distribution. Mangrove marshes are distributed along the present coastline and are usually located behind a tidal flat. Mangrove-dominated intertidal environments are quite extensive in the southeast-

Figure 6. Mangrove root systems. (A) Stilt roots of *Rhizophora* sp. (Treknature). (B) Pneumatophores roots of *Avicennia* sp. and *Sonneratia* sp. (CMP).

ern part of the Ca Mau Peninsula and along the mainland margins of the estuaries (Figure 1B). Mangroves are typically distributed from mean sea level (MSL) to highest spring tide (Alongi, 2009; Hogart, 1999), since below MSL the seedlings cannot settle and at higher levels the mangroves cannot compete with other plants (Schiereck and Booij, 1995). A succession of mangroves in the Mekong Delta is roughly described by three stages (Phan and Hoang, 1993):

Pioneer stage: is typically found on tidal flats, which are flooded by the mean tide. *Sonneratia alba* and *Avicennia alba* are pioneers because these two species can tolerate extensive floods and high salinity. Also they share the same biological characteristics and have pneumatophore roots.

Transitional stage: is recognized by a community of *A. alba* and *Rhizophora apiculata*. Propagules of *Rhizophora* are protected by the pioneer against the waves. After 4–5 years they can surpass *A. alba* and as a result the pioneer species are eliminated in the course of time.

Final stage: is only flooded with high tide and therefore includes other mangrove species, making the final stage a multispecies community.

The southern coast has favorable conditions, especially rainfall and the availability of alluvial sediment, for the growth and distribution of mangrove trees. Therefore, mangrove species are quite diverse in this area. For brevity in the numerical simulations we have divided mangrove species into two main families, *Rhizophora* sp. and *Sonneratia* sp., which means the pioneer stage is covered by *Sonneratia* sp. and the transitional stage and the final stage are covered by *Rhizophora* sp. This choice is based on the fact that mangroves are easily distinguished by their root systems, which are highly adapted to their specific habitat (Figure 6). *Rhizophora* sp. is typical for a prop root system (stilt roots) that arises from its trunk and its lower branches. *Avicennia* sp. and *Sonneratia* sp. are known by their pneumatophores, which are erect lateral branches of the horizontal cable roots, and are themselves growing underground (De Vos, 2004). *Sonneratia*, the pioneer species, is applied near the water line and *Rhizophora* sp. is applied farther inshore. Since there are no common rules for the transition from the pioneer species to the species associated with the transitional stage, it is assumed that *Sonneratia* sp. will be present from MSL to the middle of the forest (for example, $x = 1000$ m in case of 2000-m mangrove forest width) and *Rhizophora* sp. will be present from the middle to the edge of the forest at the landward side.

Xbeach Model

The effectiveness of wave attenuation by a mangrove forest depends mainly on vegetation properties and hydraulic boundary conditions as discussed by several researchers (De Vos, 2004; Burger, 2005; Meijer, 2005; Suzuki, 2011). Quite a limited number of studies on wave attenuation in the field in Vietnam have been published. Among these studies, four of them are about fringing mangrove (Bao, 2011; Mazda *et al*., 1997, 2006; Quartel *et al*., 2007), and one is about riverine mangrove at the southern coast of Vietnam (Vo-Luong and Massel, 2006). The field experiment on wave motion and suspended sediment transport of riverine mangrove at Can Gio (Vo-Luong and Massel, 2006) was used to validate a theoretical model for wave propagation through a nonuniform forest of arbitrary water depth proposed by Vo-Luong and Massel (2008). On the basis of the field observations at Tong Kinh Delta and at Vinh Quang coast, Mazda *et al*. (1997, 2006) suggested a quantitative formulation of the relationship between vegetation characteristics, water depth, and incident wave conditions. This relationship once again confirmed the field study of Quartel *et al*. (2007) on wave attenuation in coastal mangrove in the Red River Delta. Bao (2011) collected data on wave height attenuation and mangrove characteristics from 32 mangrove plots located in two coastal regions in Vietnam: the Red River Delta and Can Gio mangrove forest. This research proved the importance of sufficient mangrove bandwidth for wave height attenuation. However, in all these studies only short waves are consid-

Table 2. *Different scenarios for XBeach simulation, Soc Trang case study.*

Mangrove Width	Mangrove Density
1. No sea dike + 2000-m mangrove width	1. Spare density
2. Sea dike + 1000-m mangrove width	2. Average density
3. Sea dike + 600-m mangrove width	3. Dense density
4. Sea dike + 400-m mangrove width	
5. Sea dike + 200-m mangrove width	

ered, whereas longer waves generated by wave groups are expected to play an important role in the hydrodynamics and sediment transport processes within mangrove systems as suggested by Massel, Furukawa, and Brinkman (1999). The mildly sloped mangrove beaches and their even more gently sloping foreshores create dissipative conditions in which the incident wind and swell waves dissipate most of their energy before reaching the shoreline. At the edge of the mangrove forests the longer infragravity band will therefore already substantially contribute to the water surface variance. Within the mangrove forest this effect is enhanced since longer-period waves such as swells and infragravity waves are subject to less attenuation, whereas short-period waves with frequencies related to wind waves lose substantial energy due to stronger interactions with the vegetation. To consider the effect of both incident waves and infragravity waves, the XBeach model was used in this study to provide insight into the wave attenuation in mangrove forests and to evaluate the critical value of mangrove width as found for the east coast of Vietnam in more quantitative terms.

XBeach is a two-dimensional model for wave propagation, long waves, and mean flow. The model consists of formulations for short-wave envelope propagation, nonstationary shallow-water equations, sediment transport, and bed update. Innovations include a newly developed time-dependent wave action balance solver, which solves the wave refraction and allows variation of wave action in x, y, time, and over the directional space, and can be used to simulate the propagation and dissipation of wave groups (Roelvink *et al.*, 2009). Recently, the development team has been working on a very new application: "wave attenuation by vegetation on XBeach". Wave attenuation by vegetation is successfully implemented in the simulating waves nearshore (SWAN) model for short waves by Suzuki (2011). The implementation is based on an energy attenuation equation first provided by Dalrymple, Kirby, and Hwang (1984), which was further developed and validated by Mendez and Losada (2004):

$$D_v = \frac{1}{2\sqrt{\pi}}\rho C_{\mathrm{D}} b_v N_v \left(\frac{k}{2\sigma}\right)^3 \frac{\sinh^3 k\alpha h + 3\sinh k\alpha h}{3k\cosh^3 kh} H_{rms}^3 \qquad (1)$$

where D_v is the time-averaged rate of energy dissipation per unit area; C_{D}, b_v, and N_v are the vegetation drag coefficient, diameter, and spatial density; k is the average wave number; σ is the average wave frequency; αh is the mean vegetation height; h is the water depth (m); and H_{rms} is the significant wave height at that point (m).

In the XBeach model, the short-wave attenuation by vegetation is implemented in a comparable way, where k and σ are respectively the wave number and wave frequency associated with the peak period of the incident waves. The long-wave attenuation by vegetation is modeled with a Morrison-type equation defined as:

$$F_v = 0.5 C_D b_v N_v \frac{\alpha h}{h} u|u| \qquad (2)$$

where u is the orbital velocity.

The vegetation properties can be specified for multiple species and can vary per species over the vertical to mimic a mangrove tree. In XBeach a vegetation-file can be specified that contains a file list with vegetation properties including number of vertical sections, the height of a section (h), drag coefficient (C_{D}), number of plants per unit area (N_v), and plant area per unit height (b_v). To check the correct implementation and applicability of XBeach we have included a comparison with laboratory experiments in an Appendix.

Different Scenarios and Input Parameters

Five scenarios of mangrove width are considered, including a case without a sea dike on which mangroves are expected to healthily develop from MSL up until mean high water (MHW) (Table 2). In four other cases the mangrove width is limited by the presence of a sea dike. For each case three scenarios of mangrove density (spare density, average density, and dense density) were considered. No variations in vegetation height are taken into account since the water depth is quite small compared with the mangrove height.

The simulations discussed are executed with XBeach revision range 3234:3237 and default settings were used as much as possible. Specific settings are explained below and are related to bathymetry, hydraulic boundary conditions, and vegetation properties.

The one-dimensional cross-shore bathymetry was estimated using hydrographic maps from the Delft University of Technology map room. Three depth contours from 10 to 30 m (extending up to 100 km offshore) were digitised manually from the maps. Intermediate contours were interpolated using a simple Matlab script. The tidal levels at Mekong Delta are recorded for every hour at two stations. Hon Ba is the offshore station, located at Con Dao Island (8°38′54″ N, 106°33′18″ E). The nearshore station is located at Vung Tau (10°24′43″ N, 107°8′11″ E).The spring tidal ranges at Hon Ba and Vung Tau are 0.4–3.5 m and 0.3–3.5 m respectively. In this study the tidal range chosen is 0.4–3.5m. From this range, MSL is found to be 1.95 m. Since there is no available information about the slope of mangrove forest at Mekong Delta, the slope was estimated as follows. Mangroves are only found between MSL and MHW, which means from 1.95 m to 3.5 m above ordnance datum. Observations from Google Earth show that the mangrove width at Soc Trang coast is in the order of approximately 1500 m. Therefore the slope of the mangrove forest at Soc Trang is estimated to be about 1/1000.

The nine vegetation parameters—three for each of the three layers that had to be estimated or measured on the basis of the requirements of the XBeach model—are the diameters (b_v), densities (N_v) and heights (αh) of the roots, stem, and canopy. The characteristics of *Rhizophora* sp. and *Sonneratia* sp. are fully described by Narayan *et al.* (2011) for mangrove in India, which we have adopted here. We defend applying these parameters for mangrove species in Vietnam because of the

Table 3. *Vegetation parameters (Narayan* et al.*, 2011).*

Parameters	*Sonneratia*	*Rhizophora*
Stem diameter (m)	0.3	0.25
Root diameter (m)	0.02	0.075
Canopy diameter (m)	0.5	0.5
Stem height (m)	6	6
Root height (m)	0.5	0.8
Canopy height (m)	2	2
Density variations		
Stem (m^{-2})		
Spare	0.5	0.5
Average	0.7	0.7
Dense	1.7	1.7
Root (m^{-2})		
Spare	25	30
Average	50	60
Dense	100	130
Canopy (m^{-2})		
Spare	50	50
Average	100	100
Dense	100	100

similarities between the mangrove species in the Mekong Delta and those in India (including *Sonneratia* sp. and *Rhizophora* sp.) (Table 3).

A representative wave height to be applied as offshore boundary condition in our simulations is derived as follows. An important part of the cross-shore sediment transport rate is proportional to the odd moment $\langle u|u^2|\rangle$ (Bosboom and Stive, 2011), where u is the instantaneous cross-shore velocity and the brackets indicate time averaging. The term u^2 can be interpreted as representing the sediment concentration stirred up by the oscillatory wave motion. In shallow water this motion is proportional to the wave height. This we have used to derive a representative wave height by weighing the square of the wave height with its frequency of occurrence, which resulted in a representative offshore wave height of 3 m.

RESULTS

Here we discuss the results of our simulations of wave transformation from offshore to nearshore for the various cases considered. The reference case is a situation with no mangroves, which is compared with various mangrove density cases. Finally, the effect of a sea dike at various distances from the waterline is discussed.

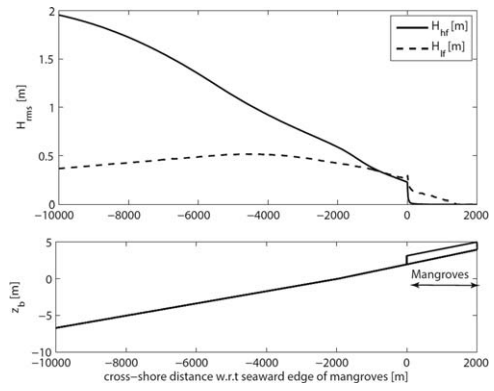

Figure 7. Example of wave height transmission from offshore to nearshore in case of 2000-m mangrove width; H_{rms} is the root mean square wave height and z_b is the bed level, relative to MSL.

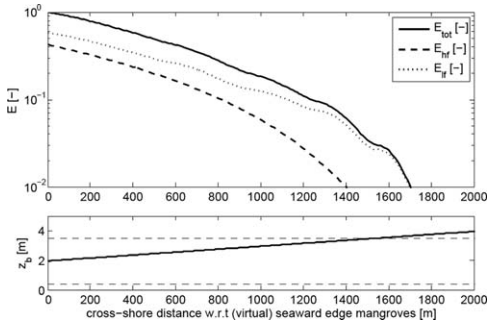

Figure 8. Normalized wave energy transformation in case of no mangrove, in which E_{tot} is the total wave energy, E_{hf} is the high-frequency energy or short-wave energy, E_{lf} is the low-frequency energy or long-wave energy, and z_b is the bed level.

Wave Transformation from Offshore to Nearshore

The wave height transmission for both long and short waves from offshore to nearshore is shown in Figure 7. Because of wave breaking, the short wave height (H_{hf}) decreases gradually to less than 0.5 m at the seaward edge of the mangrove forests. The long wave height (H_{lf}) first slightly increases toward the shoreline until $x = -4000$ m and then starts to decrease slowly. At the seaward edge of the mangroves the long wave height exceeds the short wave height.

Wave Transformation without Mangrove

Figure 8 shows the normalized wave energy transformation over a profile without mangrove. The vertical axis shows the normalized wave energy and the horizontal axis shows the cross-shore distance with respect to the shoreline position at MSL (this location is commonly associated with the seaward edge of mangrove vegetation). The normalized wave energy at a specific location x is defined as the ratio between the wave energy at this location divided by the wave energy at $x = 0$ and is a measure for attenuation. It can be seen from Figure 8 that at $x = 0$ 60% of the incoming wave energy is in the long waves (E_{lf}) and only 40% of the energy is in the short waves (E_{hf}). On the basis of this finding it is anticipated that the penetration of long waves cannot be neglected in understanding mangrove hydrodynamics.

Wave Transformation in Case of Different Mangrove Densities

The wave transformation in a 2000-m-wide mangrove forest is examined for sparse, average, and dense vegetation. The results are presented in Figure 9 and show an overall increase in the degree of wave attenuation from low to high vegetation density. Splitting out the overall wave height transformation (upper panel) into the attenuation of short waves (middle panel) and long waves (lower panel), respectively, reveals some interesting insights. First, the mangrove forest is very effective in attenuating the short-wave energy, which is in line with previous studies about short-wave attenuation into the

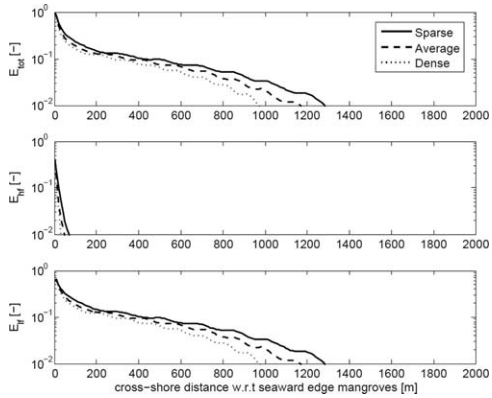

Figure 9. Normalized wave energy transformation in case of different mangrove density.

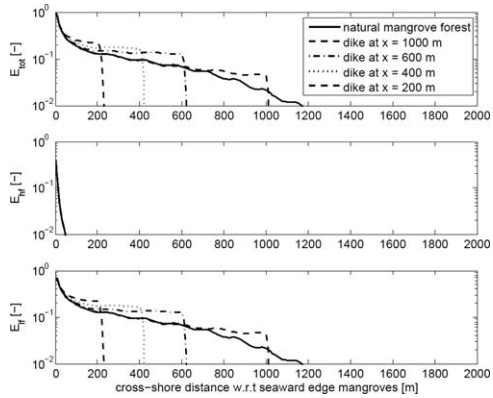

Figure 10. Effect of sea dike location on normalized wave energy transformation in case of average mangrove density.

mangrove forests (De Vos, 2004; Burger, 2005; Meijer, 2005). The short waves rapidly decrease after entering the mangrove forest and reduce until less than 1% of the incoming wave height is within the first 100 m, independent of the vegetation density. The long waves, on the other hand, are attenuated much less effectively by the vegetation and they can penetrate 950–1300 m into the forest depending on the vegetation density. We note that at a distance of 300 to 400 m the long-wave energy is 10% of that at the start of the forest. As a result the hydrodynamics farther into the mangrove forest are controlled by the tide and long waves (tidal variance not shown here).

Another observation in Figure 9 is that the long-wave height transformation shows modulations in wave height where the length scale of the modulations seems to be related to the vegetation density and increases for lower-density waves. We hypothesize that long-wave reflection both at the shoreline and on the vegetation stems is responsible for creating these modulations.

Effect of a Dike in the Profile (for Average Mangrove Density)

The presence of a sea dike can limit the width of a mangrove forest from the landward side and its presence is expected to play an important role in the stability of mangrove forests. The influence of five different sea dike locations on wave transformation into the mangrove forest is presented in Figure 10. On the basis of this figure, it seems that the short-wave transformation is independent of the cross-shore location of the dike since all incident band energy is attenuated by the mangrove within 50 to 100 m. The long-wave height transformation instead is strongly affected by the cross-shore location of the dike. The more seaward the dike the higher the long-wave variance, which is likely related to long-wave reflections on the sea dike.

CONCLUSION

Since the past few decades erosion has been observed at various locations along the southern coast of the Mekong Delta, where sedimentation has been observed in the past. Planting mangrove forest is so far the best solution to mitigate coastal erosion in the southeastern coast and the eastern coast of the MDRS since the coast is rich in sediment supply from the Mekong River system. Mangroves can reduce wave energy and trap sediment, and therefore enhance sedimentation. It was found that the southeastern coast and the eastern coast of the MDRS was stable with a mangrove width range of approximately 30 to 250 m and 140 m on average. This result is estimated on the basis of our empirical relationship of mangrove forest width and coastline evolution from 1989 to 2002.

Results from the XBeach model for the Soc Trang case study show the effectiveness of short-wave attenuation in a mangrove forest. After passing through less than 100 m of mangrove width, the short-wave height is significantly reduced to virtually zero. Therefore it is hypothesized that short waves do not really play a role in the health of a mangrove forest.

Long waves, on the other hand, need more distance for attenuation. Even for the case of dense mangrove, long waves can still penetrate in the order of 1000 m into the forest, but after 300 to 400 m the long-wave energy is only 10% of the wave height at the seaward edge of the mangroves. A qualitative explanation could be that the long-wave energy needs to be attenuated (reflections should be limited) to create a sedimentation-friendly environment. In addition, wave reflections will potentially increase long-wave energy within the mangrove forest, dependent on the position of a sea dike.

We hypothesize that long waves play an important role in creating a favorable environment for seedlings and sedimentation. Future work will concentrate on validating our model results by both fieldwork and laboratory experiments, both in terms of hydrodynamics and of sedimentation.

ACKNOWLEDGMENTS

This study is supported by the Netherlands Initiative for Capacity development in Higher Education (NICHE) scholarship, the Netherlands; the Technical University Delft, the Netherlands; the Southern Institute of Water Resources Research of Vietnam; and the Water Resources University Ha Noi, Vietnam.

LITERATURE CITED

Alongi, D.M., 2002. Present state and future of the world's mangrove forest. *Environmental Conservation,* 29(3), 331–349.

Alongi, D.M., 2009. *The Energetics of Magrove Forests*. Queensland, Australia: Springer, 216p.

Bao, T.Q., 2011. Effect of mangrove forest structures on wave attenuation in coastal Vietnam. *Oceanologia,* 53(3), 807–818.

Bosboom, J. and Stive, M.J.F., 2011. *Coastal Dynamics I*. Delft, the Netherlands: VSSD, 573p.

Burger, B., 2005. Wave Attenuation in Mangrove Forests. Delft, the Netherlands: Delft University of Technology, Master's thesis, 73p. http://repository.tudelft.nl/view/ir/uuid%3A0e4c6450-fe5d-4693-9ca9-58da343448b7/.

Christensen, S.M.; Tarp, P., and Hjortso, C.N., 2008. Mangrove forest management planning in coastal buffer and conservation zones, Vietnam: a multimethodological approach incorporating multiple stakeholders. *Ocean and Coastal Management*, 51(10), 712–726.

CMP. The Conservation Measures Partnership. http://www.conservationmeasures.org/initiatives/threats-actions-taxonomies/actions-taxonomy/attachment/mangroves-pohnpei-micronesia.

Dalrymple, R.; Kirby, J., and Hwang, P., 1984. Wave diffraction due to areas of energy dissipation. *Journal of Waterway, Port, Coastal and Ocean Engineering*, 110(1), 67–69.

De Vos, W.J., 2004. Wave Attenuation in Mangroves Wetlands, Red River Delta, Vietnam. Delft, the Netherlands: Delft University of Technology, Master's thesis, 107p. http://repository.tudelft.nl/view/ir/uuid%3A4d8f93b5-8efa-4663-a29a-448a50c45525/.

Doody, J., 2004. 'Coastal squeeze'—an historical perspective. *Journal of Coastal Conservation,* 10(1), 129–138.

Duke, N.C., 1992. Mangrove floristics and biogeography. *In:* Robertson, A.I., and Alongi, D.M. (eds.), *Tropical Mangrove Ecosystems*. Washington, DC: American Geophysical Union, pp. 63–100.

Ewel, K.C.; Twilley, R.R., and Ong, J.E., 1998. Different kinds of mangrove forest provide different good and sevices. *Global Ecology and Biogeography Letters,* 7(1), 83–94.

Feagin, R.A.; Martinez, M.L.; Mendoza-Gonzalez, G., and Costanza, R., 2010. Salt marsh zonal migration and ecosystem service change in response to global sea level rise: a case study from an urban region. *Ecology and Sociaty,* 15(4), 1–14.

Gilman, E.; Ellison, J., and Coleman, R., 2007. Assesment of mangrove response to projected relative sea-level rise and recent historical reconstruction of shoreline position. *Environmental Monitoring and Assessment,* 124(1–3), 105–130.

Hoang, V.H. and Nguyen, H.N., 2006. Result on study of wave field on Dong Nai, Sai Gon estuaries and suggestion of sea bank and river mouth protection methods. *Proceedings of theVietnam–Japan Estuary Workshop (Ha Noi, Vietnam),* pp. 140–150.

Hogart, P.J., 1999. *The Biology of Mangroves*. Oxford, U.K.: Oxford University Press, 228p.

International Union for Conservation of Nature, 2011. *Why Healthy Ecosystems Matter: The Case of Mangroves in the Mekong Delta*. http://iucn.org/about/union/secretariat/offices/asia/regional_activities/building_coastal_resilience/?8865/Why-healthy-ecosystems-matter-the-case-of-mangroves-in-the-Mekong-delta.

Lu, X.X. and Siew, R.Y., 2006. Water discharge and sediment flux changes over the past decades in the Lower Mekong River: possible impact of the Chinese dams. *Hydrology and Earth System Sciences,* 10(2), 181–195.

Lugo, A.E., and Snedaker, S.C., 1974. The ecology of mangroves. *Annual Review of Ecology and Systematics,* 5(1), 39–64.

Massel, S.R.; Furukawa, K., and Brinkman, R.M., 1999. Surface wave propagation in mangrove forests. *Fluid Dynamic Research*, 24(4), 219–249.

Mazda, Y.; Magi, M.; Ikeda, Y.; Kurokawa, T., and Asano, T., 2006. Wave reduction in a mangroves forest dominated by *Sonneratia* sp. *Wetlands Ecology and Management,* 14(4), 365–378.

Mazda, Y.; Magi, M.; Kogo, M., and Hong, P.N., 1997. Mangroves as a coastal protection from waves in the Tong Kinh Delta, Vietnam. *Mangroves and Salt Marshes,* 1(2), 127–135.

Meijer, M.C., 2005. Wave attenuation over salt marsh vegetation. Delft, the Netherlands: Delft University of Technology, Master's thesis, 95p. http://repository.tudelft.nl/view/ir/uuid%3A60eddf18-2289-47f5-b76c-5e989a1167ff/.

Mendez, F.J. and Losada, I.n.J., 2004. An empirical model to estimate the propagation of random breaking and nonbreaking waves over vegetation fields. *Coastal Engineering*, 51(2), 103–118.

Narayan, S.; Suzuki, T.; Stive, M.J.; Verhagen, H.; Ursem, W., and Ranasinghe, R., 2011.On the effectiveness of mangroves in attenuating cyclone-induced waves. Coastal Engineering Proceedings, 1(32), waves.50. doi:10.9753/icce.v32.waves.50.

Nguyen, V.L.; Ta, T.K.O., and Tateishi, M., 2000. Late Holocene depositional environments and coastal evolution of the Mekong River Delta, southern Vietnam. *Journal of Asian Earth Science*, 18(4), 427–439.

Phan, N.H. and Hoang, T.S., 1993. *Mangroves of Vietnam*. Bangkok, Thailand: IUCN, 173p.

Quartel, S.; Kroon, A.; Augustinus, P.G.E.F.; Van Santen, P., and Tri, N.H., 2007. Wave attenuation in coastal mangroves in the Red River Delta, Vietnam. *Journal of Asian Earth Sciences,* 29(4), 576–584.

Roelvink, D.; Reniers, A.; van Dongeren, A.; van Thiel de Vries, J.S.M.; McCall, R., and Lescinski, J., 2009. Modelling storm impacts on beaches, dunes and barrier islands. *Coastal Engineering*, 56(11–12), 1133–1152.

Schiereck, G.J. and Booij, N., 1995. Wave transmission in mangrove forest. *Proceedings of the International Conference in Coastal and Port Engineering in Developing Countries* (Rio de Janeiro, Brazil), pp. 1969–1983.

Southern Institute of Water Resources Research, 2005. *Summary Report KC08* [in Vietnamese]. Ho Chi Minh, Vietnam: Ministry of Agriculture and Rural Development of Vietnam, 210p.

Spalding, M.; Kainuma, M., and Collins, L., 2011. *World Atlas of Mangroves*. London: Earthscan, 319p.

Stive, M.J.F.; Aarninkhof, S.G.; Hamm, L.; Hanson, H.; Larson, M., and Wijnberg, K.M., 2002. Variability of shore and shoreline evolution. *Coastal Engineering,* 47(2), 211–235.

Suzuki, T., 2011. Wave Dissipation over Vegetation Fields. Delft, the Netherlands: Delft University of Technology, Ph.D. thesis, 175p. http://repository.tudelft.nl/view/ir/uuid%3Aff8147df-4389-4394-bf0c-3fe50076e557/

Ta, T.K.O.; Nguyen, V.L.; Tateishi, M.; Kobayashi, I.; Saito, Y., and Nakamura, T., 2002. Sediment facies and Late Holocene progradation of the Mekong River Delta in Ben Tre Province, southern Vietnam: an example of evolution from a tide-dominated to a tide- and wave-dominated delta. *Sedimentary Geology*, 152(3–4), 313–325.

Torio, D.D. and Chmura, G.L., 2013. Assessing coastal squeeze of tidal wetlands. *Journal of Coastal Research,* 29(5), 1049–1061.

TREKNATURE. http://www.treknature.com/gallery/photo1937.htm.

Tri, V.K., 2012. Hydrology and hydraulic infrastructure system in the Mekong Delta, Vietnam. *In:* Renaud, F.G. and Kuenzer, C. (eds.), *The Mekong Delta System: Interdisciplinary Analyses of a River Delta*. Heidelberg, Germany: Springer, pp. 49–81.

Vo-Luong, H.P. and Massel, S.R., 2006. Experiment on wave motion and suspended sediment concentration at Nang Hai, Can Gio mangrove forest, southern Vietnam. *Oceanologia,* 48(1), 23–40.

Vo-Luong, H.P. and Massel, S.R., 2008. Energy dissipation in non-uniform mangrove forests of arbitrary depth. *Journal of Marine Systems,* 74(1–2), 603–622.

Woodroffe, C.D., 1992. Mangrove sediments and geomorlogy. *In:* Robertson, A.I. and Alongi, D.M. (eds.), *Tropical Mangrove Ecosystems*. Washington, DC: American Geophysical Union, pp. 7–41.

APPENDIX

The XBeach model was recently extended to simulate short- and long-wave attenuation by vegetation. To validate the implementation the numerical result of short-wave attenuation over vegetation is compared with the experimental results of Suzuki (2011). The most relevant cases are the two flat-bottom cases with irregular incoming waves. In this

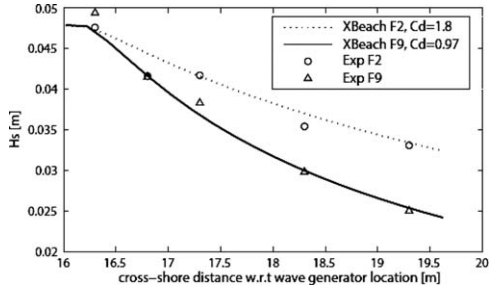

Figure A1. Short-wave attenuation over vegetation is validated on the basis of Suzuki's experiment (2011).

experiment rigid artificial vegetation was used, made of smooth plywood cylinders with diameter $D = 0.6$ cm, cylinder height $h_{veg} = 10$ cm, and densities of 242 units/m^2 (case F2) and 962 units/m^2 (case F9). The input parameters are given in Table A1, in which $h = 0.1$ m is the water depth at the impermeable flat bottom. Wave period T and wave height H_I are input values for the wave generation.

Figure A1 shows the experiment results and numerically calculated short-wave heights in two chosen cases F2 and F9.

Table A1. *A set of flat bottom cases (Suzuki, 2011).*

Case Name	Wave	h (m)	H_I (cm)	T (s)	C_D
F2I100516	Irregular	0.1	5.0 (H_s)	1.6 (T_p)	1.35
F9I100516	Irregular	0.1	5.0 (H_s)	1.6 (T_p)	0.8

The vertical axis shows the wave-height attenuation and the horizontal axis shows the distance from the wave generation. The vegetation is located from $x = 16.3$ m to $x = 19.3$ m.

As shown in Figure A1, it is confirmed that the wave height calculated by the numerical model is in good accordance with the flume experiment of Suzuki (2011). It has to be noted that there is a difference in drag coefficients that are used in XBeach model and in Suzuki's results. The drag coefficients are $C_D = 1.8$ and $C_D = 0.97$ in case F2 and case F9 respectively with XBeach model, differing only 10 to 20% from those used by Suzuki. These differences of the drag coefficients used in the XBeach model and in Suzuki's results are not significant and are acceptable. Drag coefficients from Suzuki's result are obtained from the SWAN calculations. XBeach and SWAN have different approaches to calculate wave-height attenuation therefore it might create a slightly different drag coefficient than that used by each model.